Electronic Supplementary Material (ESI) for New Journal of Chemistry.

Supplementary Information

Controllable Dispersion of Cobalt Phthalocyanine Molecules on Graphene Oxide for Enhanced Electrocatalytic Reduction of CO_2 to CO

Weifeng Huang,[abc] Junqiang Li,[abc] Xiao Xu,[bc] Aihui Cao,[bcd] Ying He,[bcd] Miao Sun[bc] and Longtian Kang*[bcd]

a College of Chemistry, Fuzhou University, Fuzhou 350108, P. R. China

b Key Laboratory of Design and Assembly of Functional Nanostructures, and Fujian Provincial Key Laboratory of Nanomaterials, Fujian Institute of Research on the Structure of Matter, Chinese Academy of Sciences, Fuzhou, Fujian 350002, P. R. China.

c Fujian Science & Technology Innovation Laboratory for Optoelectronic Information of China, Fuzhou, Fujian 350108, P. R. China.

d University of Chinese Academy of Sciences, Chinese Academy of Sciences, Beijing, 100049, P. R. China.

**Corresponding author at: Fujian Institute of Research on the Structure of Matter, Chinese Academy of Sciences, Fuzhou, Fujian 350002, P. R. China. E-mail: longtiank@fjirsm.ac.cn*

Materials characterization

High-resolution field emission scanning electron microscope (SEM) of all samples was measured using the Hitachi SU8010. The structure and element distribution of samples were characterized by transmission electron microscope (TEM, FEI F20). X-ray photoelectron spectroscopy (XPS) characterization was accomplished on an ESCALAB 250Xi instrument using an Al Kα radiation exciting source. X-ray powder diffraction (XRD) data were obtained on a MiniFlex diffractometer (MiniFlex600, Rigaku) with Cu K_{α} radiation (λ = 1.54 Å). Fourier transform infrared spectroscopy (FT-IR) spectra were carried out via a VERTEX70 spectrometer. Raman spectra were recorded by a Lab RAM HR spectrometer (Horiba Jobin Yvon) with a laser of 532 nm.

Electrocatalytic measurement of CO_2RR

The electrochemical measurement was performed with an electrochemical workstation (CHI760E) from Shanghai Huachen. The reference and counter electrodes used for the experiments were Ag/AgCl (saturated KCl solution) electrode and Pt net (1x1 cm^2). 80 μL of dispersion was evenly applied to both sides of the carbon paper (loading mass: 0.2 mg cm^{-2}). Carbon paper is clamped to the working electrode clamp. Nafion membranes are used to separate the cathode and anode. And a relative air tightness H-type electrolytic cell is employed as the electrochemical reduction reaction device. CO_2 flow was applied to the cathode chamber with a rate of 20 sccm and analyzed by gas chromatograph (GC-2014). CO_2 was continuously purged for 30 min and then linear scanning voltammetry (LSV) was executed at 10 mV s^{-1} from 0 to −1.2 V relative to the reversible hydrogen electrode (vs. RHE). To determine the Faradaic efficiency, a multi-potential step (STEP) potential electrolysis was performed at 90% IR compensation. The i-t curve remained stable after 750 s. Then 1 mL of gaseous product was captured and detected by gas chromatography. In addition, we use the average steady current density during 750 s as the jtotal current to calculate J_{co}, which is more accurate. Electrochemical impedance spectroscopy (EIS) was performed in 0.1 M $KHCO_3$ with an AC voltage amplitude of 5 mV and a frequency of 0.1 Hz to 100 KHz to study the charge transfer resistance.

Surface concentration of electrochemically active Co sites was calculated as follows:

$$f = \frac{n}{n_{tot}}$$

$$n = \frac{Q}{F}$$

$$\mathrm{Q} \;=\; \frac{A\times s}{\text{Ʋ}}$$

$$n_{tot} \;=\; \frac{m\times W_{Co}}{M}$$

ʃ: surface concentration of electrochemically active Co sites.

n: the amount of surface active Co on the working electrode.

n_{tot}: the total amount of surface active Co on the working electrode.

Q: the integrated charge of the anodic wave.

F: Faraday constant (96485 C/mol).

A: the anodic wave area in the Ar CV curve.

S: Loading area on the working electrode.

m: the mass of the electrocatalyst loaded on the working electrode.

Ʋ: Co^{I}/Co^{II} redox region scanning rate (V/s).

W_{Co}: the weight fraction of Co in the electrocatalyst determined from the ICP analysis.

M: the atomic weight of Co (58.93 g/mol) .

Turnover frequency (TOF) is defined as the mole of reduction product generated per electrocatalytic active site per unit time. Turnover number (TON) is defined as the mole of reduction product generated per electrocatalytic active site over a given period of time. TOF and TON are calculated as follows:

$$\mathrm{TOF} = \frac{TOF_0}{\text{ʃ}} = \frac{j_{tot}\times FE_{CO}(\%)}{2F\times n_{tot}\times \text{ʃ}}$$

$$\mathrm{TON} \;=\; \frac{Q\times \mathrm{FE}_{CO(average)}}{2F\times n_{tot}\times f}$$

Q: the total reduction charge pass during the 10000 s bulk electrocatalysis.

$FE_{CO(average)}$: the estimated average CO faradaic efficiency during the bulk electrocatalysis.

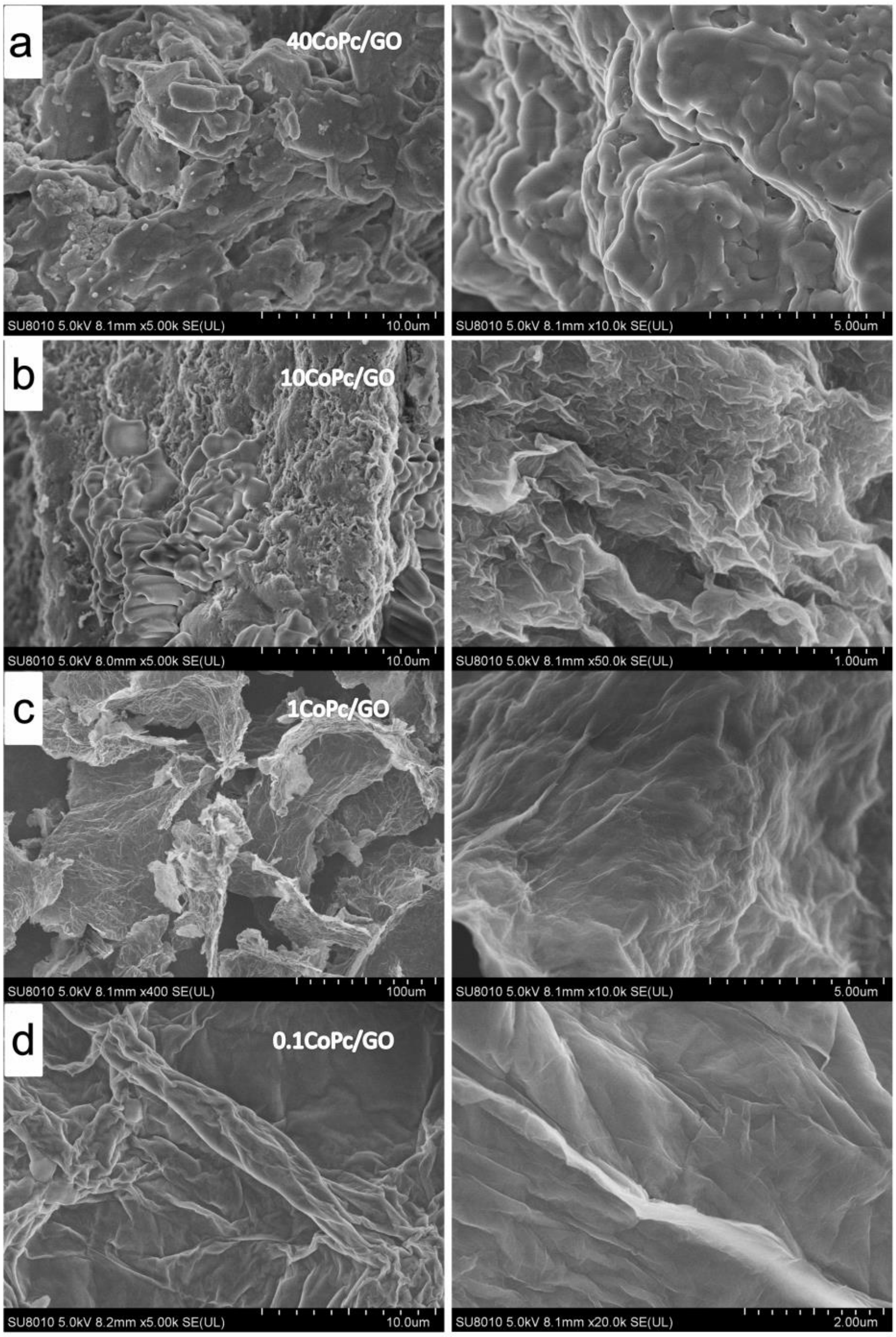

Fig. S1 (a-d) SEM images of 40CoPc/GO, 10CoPc/GO, 1CoPc/GO, and 0.1CoPc/GO composites.

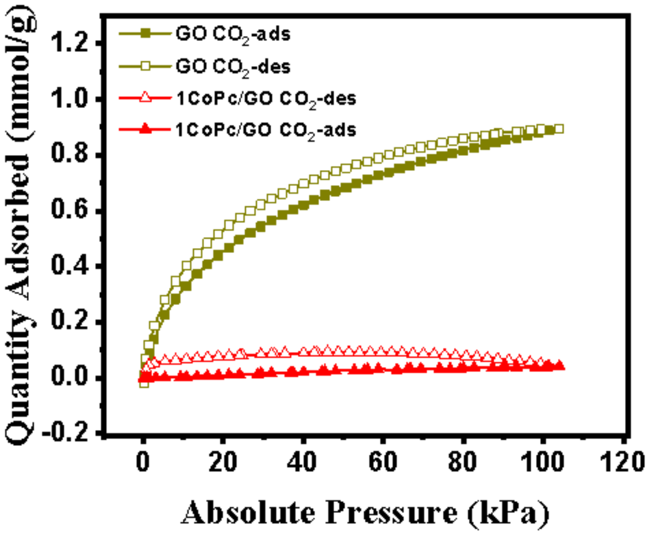

Fig. S2 CO_2 adsorption-desorption isotherms at 295 K of the 1CoPc/GO, GO.

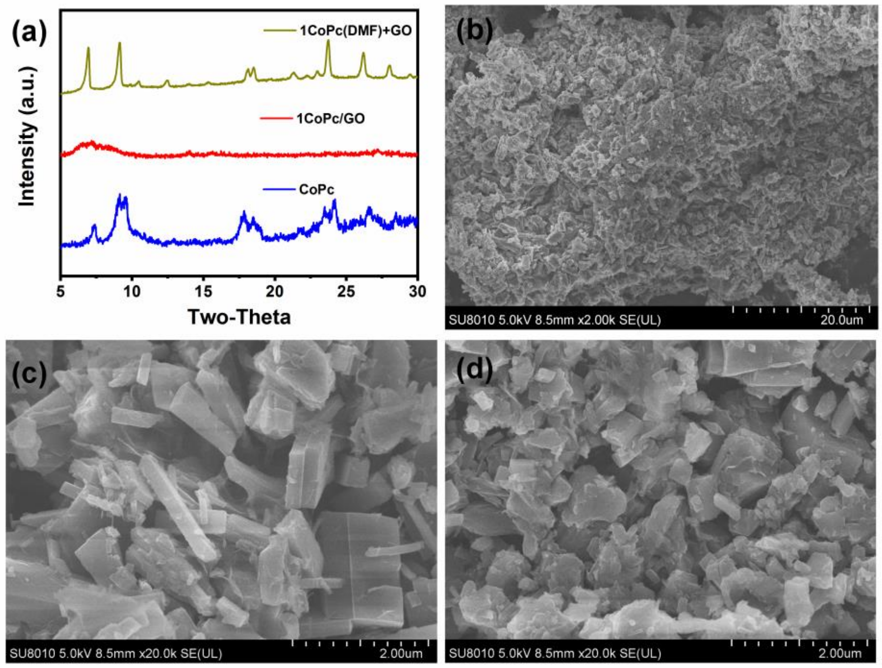

Fig. S3 (a) XRD patterns of 1CoPc(DMF)+GO, 1CoPc/GO and CoPc. (b-d) SEM images of 1CoPc(DMF)+GO.

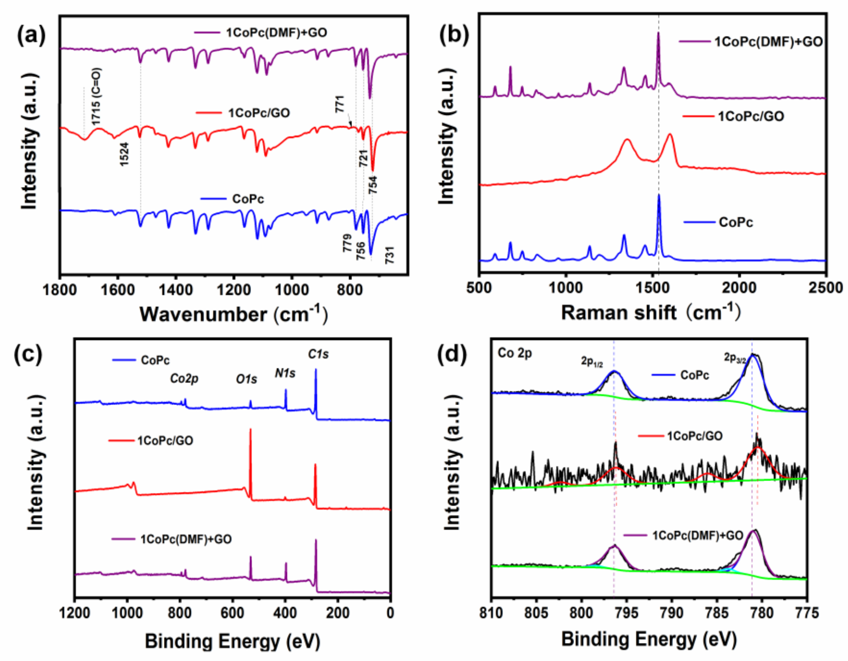

Fig. S4 (a) FT-IR and (b) Raman spectra of 1CoPc(DMF)+GO, 1CoPc/GO and CoPc. (c) Survey spectra of XPS, and (d) High resolution XPS spectra of Co 2p.

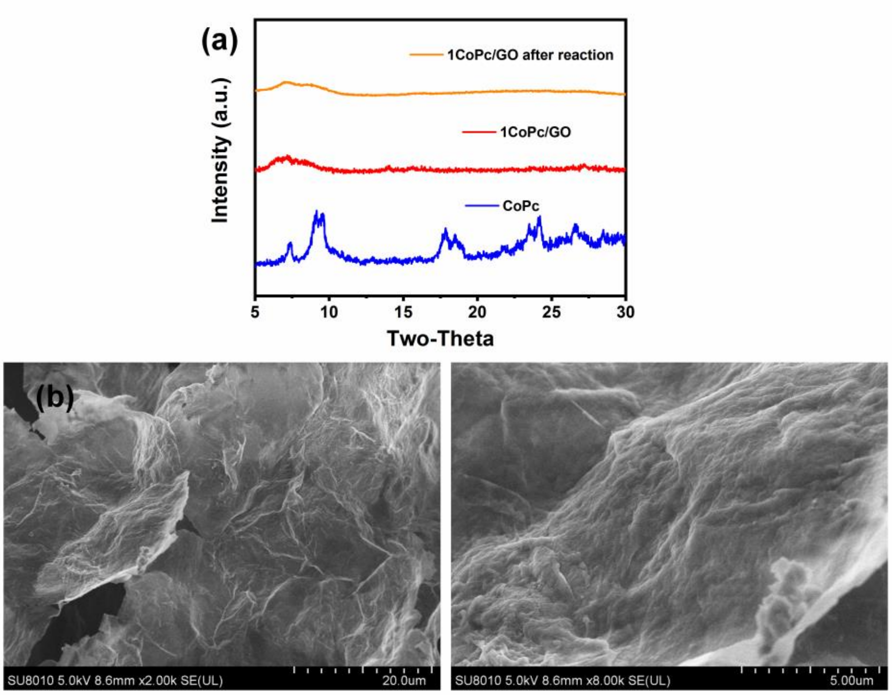

Fig. S5 (a) XRD patterns and (b) SEM images of 1CoPc/GO composites after CO_2RR test.

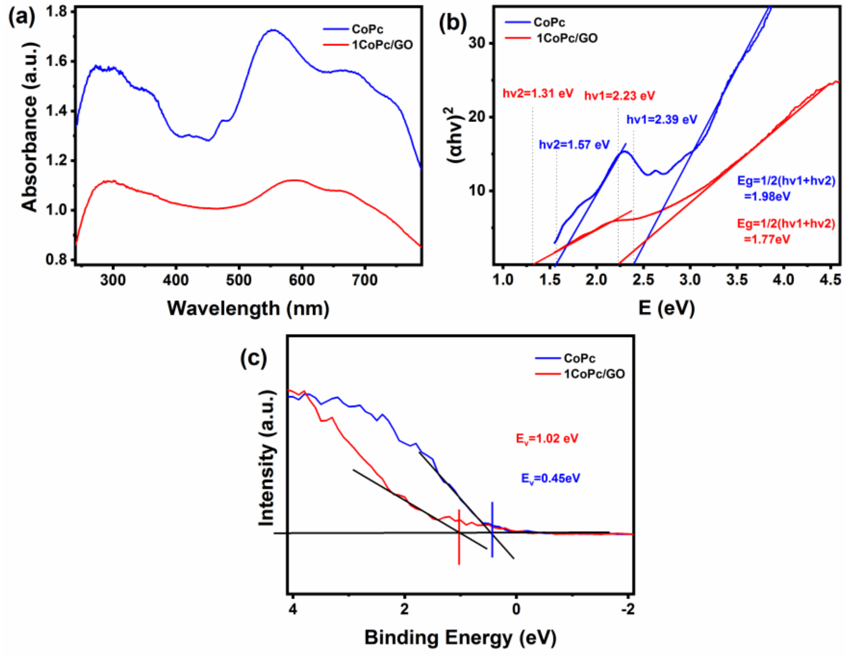

Fig. S6 (a) Solid-state UV-Vis spectrum, (b) The band gap calculation from the UV-Vis spectrum and (c) VB XPS plots of 1CoPc/GO and CoPc.

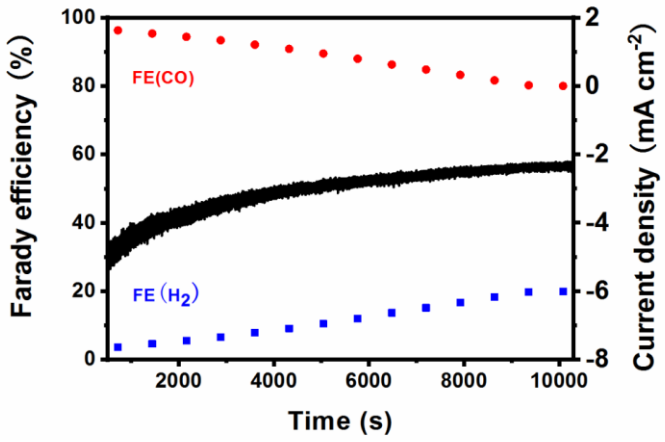

Fig. S7 Stability test of 1CoPc/GO at −0.9 V vs RHE and the corresponding Farady efficiency of CO and H_2.

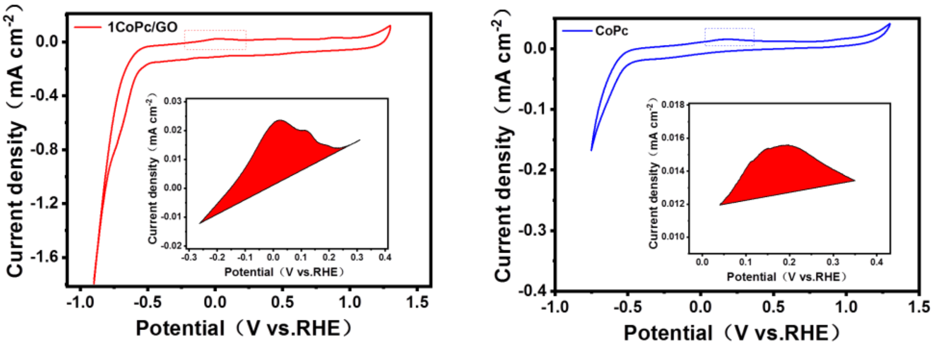

Fig. S8 CV curve of 1CoPc/GO and CoPc in Ar-saturated 0.1 M $KHCO_3$. Insert shows the total charge integrated from the Co^I/Co^{II} anodic wave.

We integrated the anodic wave in the CV curve of 1CoPc/GO and CoPc. The weight fraction of Co in 1CoPc/GO and CoPc electrocatalyst by ICP analysis and then calculated the amount of surface active Co by assuming a one-electron redox process:

$$\mathrm{n}_{1CoPc/GO} = \frac{Q}{F} = \frac{3.18\ mC}{96485\ C/mol\times 1000} = 3.30\times 10^{-8}\ mol$$

$$\mathrm{n}_{CoPc} = \frac{Q}{F} = \frac{1.79\ mC}{96485\ C/mol\times 1000} = 1.85\times 10^{-8}\ mol$$

$$\text{1CoPc/GO :}\ \mathrm{n_{tot}} = \frac{\mathrm{0.4mg\times 2.7\%}}{58.93\ g.mol^{-1}} = 1.83\times 10^{-7}\ mol$$

$$f = \frac{n}{n_{tot}} = \frac{3.3\times 10^{-8} mol}{1.83\times 10^{-7} mol}\times 100\% = 18\%$$

$$\text{CoPc :}\ n_{tot} = \frac{\mathrm{0.4mg\times 8.54\%}}{58.93\ g.mol^{-1}} = 5.8\times 10^{-7}\ mol$$

$$f = \frac{n}{n_{tot}} = \frac{1.85\times 10^{-8} mol}{5.8\times 10^{-7} mol}\times 100\% = 3.2\%$$

1CoPc/GO has a surface active Co site ratio of 18% with more effective active Co sites than CoPc (ƒ=3.2%). More active Co atom will enhance the electrocatalytic CO_2 performance, which is consistent with our result.

Let's take the calculation of TOF at −0.9 V as an example, assuming that all Co sites are involved in CO_2RR electrocatalysis:

$$\text{1CoPc/GO :}\ \mathrm{TOF} = \frac{j_{tot}\times FE_{CO}(\%)\times S}{2F\times n_{tot}\times f} = \frac{3.46 mA.cm^{-2}\times 2cm^2\times 96\%}{2\times 96485 C/mol\times 1.83\times 10^{-7} mol\times 18\%} = 3757\ h^{-1}$$

$$\text{CoPc}: \ \mathrm{TOF} = \frac{j_{tot\times FE_{CO}(\%)\times S}}{2F\times n_{tot}\times \text{ʃ}} = \frac{0.95 mA.cm^{-2}\times 2cm^{2}\times 79\%}{2\times 96485C/mol\times 5.8\times 10^{-7}mol\times 3.2\%} = 1510\ h^{-1}$$

In study, bulk electrocatalysis was performed at −0.9 V for 10000 s. TON was first calculated by assuming that all Co sites were involved in CO_2RR electrocatalysis:

$$\mathrm{TON} = \frac{Q\times \mathrm{FE}_{CO(average)}}{2F\times n_{tot}\times f} = \frac{64.88\ C\times 88.3\%}{2\times 96485\times 1.83\times 10^{-7}\times 18\%} = 9171$$

Table S1 w_{Co}, ʃ, ToF and TON of 1CoPc/GO and CoPc.

−0.9 V	w_{Co}	ʃ	TOF	TON
1CoPc/GO	2.7%	18%	3757	9171
CoPc	8.54%	3%	1510	3350

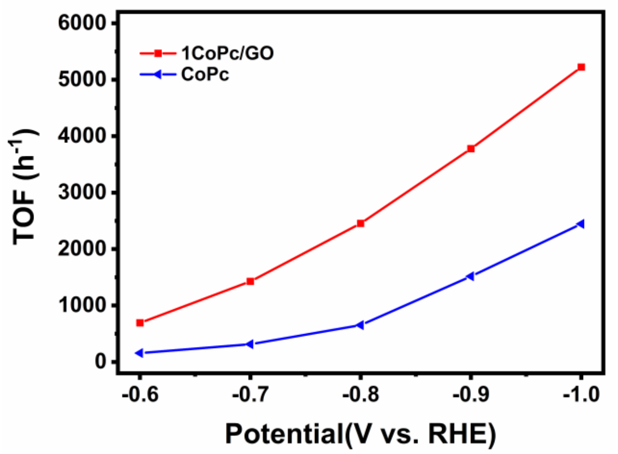

Fig. S9 TOF of the 1CoPc/GO and CoPc under different voltage.

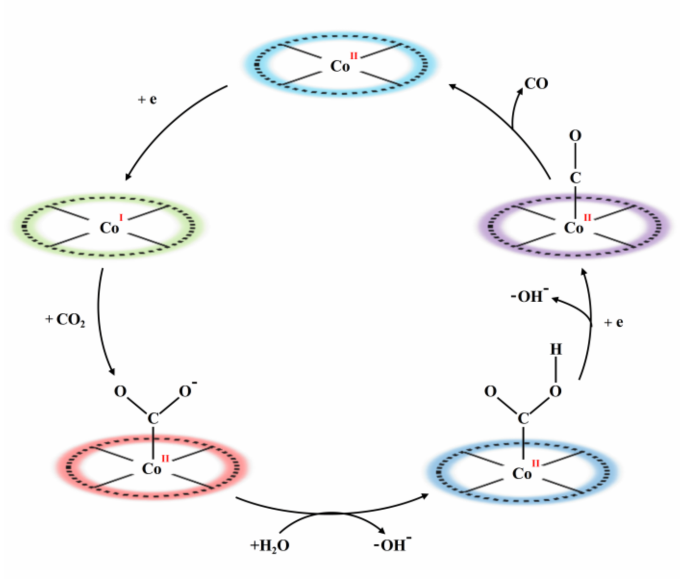

Fig. S10 Proposed mechanistic scheme for the electrochemical CO_2RR on 1CoPc/GO.

Table S2 Summary of electrocatalytic performance of cobalt-based materials for CO_2RR to CO

Catalyst	**Electrolyte (V versus RHE)**	***j***	**Faradaic Efficiency (potential range FE_{CO}>90%)**	**TOF**	**Ref**
1CoPc/GO	0.1 M $KHCO_3$ (-0.9 V)	3.46 mA/cm^2 0.2 mg/cm^2	>96% (~0.4 V, -0.7 V to -1.0V)	3757 h^{-1}	**This work**
CoFPc	0.1 M $KHCO_3$ (-0.7 V)	2.7 mA/cm^2 4.5 mg/cm^2	~93% (~0.2 V, -0.7 V to -0.8V)	3564 h^{-1}	1
CoPc-CN/CNT	0.5 M $KHCO_3$ (-0.46 V)	5 mA/cm^2 0.4 mg/cm^2	88% /	1.4 s^{-1}	2
CoPPc/CNT	0.5 M $KHCO_3$ (-0.46 V)	5.6 mA/cm^2 1 mg/cm^2	80% /	4896 h^{-1}	3
CoPcTAPc-ZIF-90	0.5 M $NaHCO_3$ (-0.97 V)	11.7 mA/cm^2 0.24 mg/cm^2	90% (~0.1 V, -0.97 V)	/	4
D-P-CoPc	0.5 M $KHCO_3$ (-0.61 V)	2.45 mA/cm^2 1 mg/cm^2	~97% (~0.1 V, -0.61V)	412 h^{-1}	5
CoPc-P4VP	0.1M NaH_2PO_4 (-0.73 V)	2.0 mA/cm^2 0.18 mg/cm^2	89% /	4.8 s^{-1}	6

CoPc/CNT	0.1 M $KHCO_3$ (-0.63 V)	9 mA/cm^2 0.4 mg/cm^2	92% (~0.14 V, -0.59 V to -0.63V)	2.7 s^{-1}	2
CoTPP-CNT	0.5 M $KHCO_3$ (-1.1V)	3.2 mA/cm^2 0.23 mg/cm^2	91% (~0.1 V, -1.1 V)	280 h^{-1}	7
N-C-CoPc	0.1 M $KHCO_3$ (-0.7 V)	25.59 mA/cm^2 0.1 mg/cm^2	85.3% /	11.35 s^{-1}	8
CoF-367-Co	0.5 M $KHCO_3$ (-0.67 V)	3.3 mA/cm^2 13 mA/mg	91%	3901 h^{-1}	9
CoF-366-Co	0.5 M $KHCO_3$ (-0.67 V)	1.8 mA/cm^2 7 mA/mg	90%	1352 h^{-1}	9

Table S3 Summary of the CO_2RR performances on CO yield.

Catalyst	**Electrolyte**	**catalyst loading**	**Rate (V versus RHE)**	**Ref**
1CoPc/GO	0.1M $KHCO_3$	0.2 mg/cm^2	0.0172 μmol. s^{-1}. cm^{-2} (-0.9 V)	**This work**
D-P-CoPc	0.5M $KHCO_3$	1 mg/cm^2	0.013 μmol. s^{-1}. cm^{-2} (-0.61V)	5
CoPc-CN/CNT	0.5M $KHCO_3$	0.4 mg/cm^2	0.0152 μmol. s^{-1}. cm^{-2} (-0.46V)	2
CoFPc	0.5M $KHCO_3$	4.5 mg/cm^2	0.0075 μmol. s^{-1}. cm^{-2} (-0.60V)	1
CoPc-P4VP	0.1M NaH_2PO_4	0.18 mg/cm^2	0.00624 μmol. s^{-1}. cm^{-2} (-0.73V)	6
CoF-366-Co	0.5M $KHCO_3$	0.2 mg/cm^2	0.00106 μmol. s^{-1}. cm^{-2} (-0.67V)	9
CoPc/CNT	0.1M $KHCO_3$	0.4 mg/cm^2	0.0486 μmol. s^{-1}. cm^{-2} (-0.63V)	2

References

1 N. Morlanés, K. Takanabe and V. Rodionov, *ACS Catal.*, 2016, 6, 3092–3095.

2 Zhang, X.; Wu, Z.; Zhang, X.; Li, L.; Li, Y.; Xu, H.; Li, X.; Yu, X.; Zhang, Z.;

Liang, Y.; Wang, H. Nat. Commun. 2017, 8, 14675.

3 N. Han, Y. Wang, L. Ma, J. Wen, J. Li, H. Zheng, K. Nie, X. Wang, F. Zhao, Y. Li, J. Fan, J. Zhong, T. Wu, D. J. Miller, J. Lu, S. T. Lee and Y. Li, *Chem*, 2017, **3**, 652–664.

4 Z. Yang, X. Zhang, C. Long, S. Yan, Y. Shi, J. Han, J. Zhang, P. An, L. Chang and Z. Tang, *CrystEngComm*, 2020, 22, 1619–1624.

5 H. Wu, M. Zeng, X. Zhu, C. Tian, B. Mei, Y. Song, X. L. Du, Z. Jiang, L. He, C. Xia and S. Dai, *ChemElectroChem*, 2018, **5**, 2717–2721.

6 Z. Xin, J. Liu, X. Wang, K. Shen, Z. Yuan, Y. Chen and Y. Q. Lan, *ACS Appl. Mater. Interfaces*, 2021, **13**, 54959–54966.

7 X.-M. Hu, M. H. Rønne, S. U. Pedersen, T. Skrydstrup and K. Daasbjerg, *Angew. Chemie*, 2017, **129**, 6568–6572.

8 H. L. Zhu, Y. Q. Zheng and M. Shui, *ACS Appl. Energy Mater.*, 2020, **3**, 3893–3901.

9 Lin S. et al. Science 349, 1208–1213 (2015).